



# Partitioning the primary ice formation modes in large eddy simulations of mixed-phase clouds

Luke B Hande<sup>1</sup> and Corinna Hoose<sup>1</sup>

<sup>1</sup>Karlsruhe Institute of Technology, Karlsruhe, Germany

*Correspondence to:* Luke B Hande (luke.hande@kit.edu)

## Abstract.

State of the art aerosol dependent parameterisations describing each heterogeneous ice nucleation mode, as well as homogeneous nucleation, were incorporated into a large eddy simulation model. Several cases representing commonly occurring cloud types were simulated in an effort to understand which ice nucleation modes contribute the most to total concentrations of ice crystals. The cases include a completely idealised warm bubble, semi-idealised deep convection, an orographic cloud, and a stratiform case. Despite clear differences in thermodynamical conditions in each case, the results are remarkably consistent between the different cloud types. In all the investigated cloud types and under normal aerosol conditions, immersion freezing dominates and contact freezing also contributes significantly. At colder temperatures, deposition nucleation plays little role, and homogeneous freezing is important. To some extent, the temporal evolution of the cloud determines the dominant freezing mechanism, and hence the subsequent microphysical processes. Precipitation is not correlated with any one ice nucleation mode, instead occurs simultaneously when several nucleation modes are active. Furthermore, large variations in the aerosol concentration have only a minor influence on the precipitation amount.

## 1 Introduction

Ice crystals in the atmosphere can form spontaneously through homogeneous nucleation, which becomes increasingly probable at temperatures of around  $-35^{\circ}\text{C}$  (Koop and Murray, 2016). At warmer temperatures an ice nucleating particle (INP) is required to initiate freezing. Although INPs represent a small fraction of all atmospheric aerosols (Rogers et al., 1998), they have a disproportionately large influence on mixed-phase cloud microphysics (DeMott et al., 2010). Therefore modelling ice microphysical processes accurately is necessary in order to correctly model clouds, and the myriad subsequent processes influenced by clouds.

Several pathways have been identified through which ice nucleation in the atmosphere can take place (Vali et al., 2015). Deposition nucleation occurs at cold temperatures, where water vapour is deposited directly onto an aerosol particle. Immersion and condensation freezing require the particle to be immersed in super-cooled liquid water, after which freezing occurs. Contact freezing occurs when an aerosol particle comes into contact with a super-cooled droplet, which subsequently initiates freezing. A similar mechanism called inside-out freezing has been identified, where a immersed particle comes into contact with the water-air interface which initiates freezing (Durant and Shaw, 2005). Contact freezing and inside-out freezing have long been



hypothesised to be important in areas of evaporation (Wang et al., 1978). Indeed, recent results from a modelling study support this idea (Hande et al., 2017).

Ice nucleation can be studied in a wide variety of ways (Cziczo et al., 2016), including under tightly controlled conditions in the laboratory. Recent reviews of laboratory experiments (Hoose and Möhler, 2012; Murray et al., 2012) highlight the tendency for much attention to be directed towards identifying and quantifying the ice nucleating ability of different aerosols species in each nucleation mode separately. These laboratory studies do little to elucidate the relative importance of these modes, so their atmospheric relevance is poorly understood.

Ladino et al. (2013) provide a review of experimental studies investigating contact nucleation, and go so far as to suggest it could dominate over immersion freezing for some aerosol species. Given that laboratory results suggest it is an efficient ice formation mechanism, these authors specifically pose the questions as to whether this also holds true in simulations. However in more recent experiments, Nagare et al. (2016) could not confirm a general enhancement in contact freezing compared to immersion freezing.

Modelling results from Cui et al. (2006) show that immersion freezing is the dominant pathway through which ice is formed, with contact playing little to no role. In this study, deposition nucleation was significant in the early stages of cloud development. Philips et al. (2007) use a model to also show that contact freezing has little impact on heterogeneous ice nucleation in deep convective clouds.

An analysis of trajectories from a dust dominated region showed air parcels commonly pass through ice saturated, but water sub-saturated regions, where deposition nucleation could occur (Wiacek and Peter, 2009). Later, Hoose et al. (2010) showed that immersion freezing dominates INP production, and in contrast to the previous modelling studies, contact freezing played an important role in their simulations.

In-situ and remote sensing observations have also been employed to study ice nucleation under atmospheric conditions. Ansmann et al. (2009) observed deep convective clouds which almost always had liquid water at cloud top, suggesting deposition nucleation plays little role. This has been supported by observations in cases of lee-wave clouds (Field et al., 2012) and stratiform clouds (De Boer et al., 2011; Westbrook and Illingworth, 2011), suggesting either immersion or contact freezing dominates ice production.

A recent global analysis of satellite observations (Carro-Calvo et al., 2016) indicates there are low cloud glaciation temperatures in areas of deep convection, not only in the tropics, but also extending to the mid-latitudes. This suggests homogeneous freezing and/or deposition nucleation are important. The warm ice clouds analysed in their study, on the other hand, were associated with stratiform cloud systems, and the authors pose the question of the role that dynamics plays in initiating early cloud glaciation.

Since immersion and contact freezing require the presence of liquid water, they are thought to be the dominant ice formation pathway in mixed phase clouds. The above studies seem to suggest this is the case, however there is still considerable uncertainty. In addition to this, there is little consensus on whether deposition nucleation or homogeneous freezing contribute significantly to ice production at cirrus temperatures.



A further complication arises since ice nucleation is clearly influenced by the ambient environmental conditions, and as such the dominant mode could depend on the cloud type. This paper aims to help clarify, in a systematic way, which ice nucleation modes dominate for various cloud types found over continental regions. The contribution of each mode to precipitation will also be considered. The cases studied here are a warm bubble, semi-idealised deep convection, idealised orographic, and a stratiform cloud, and hence cover a variety of thermodynamical conditions.

## 2 Model description

The non-hydrostatic regional weather forecasting model COSMO (CONsortium for Small-scale MOdelling) (Schättler et al., 2008) version 5.01 was run at high resolution of  $8.9 \times 10^{-4}$  degrees ( $\approx 100$  m). This scale is small enough to resolve energy-containing turbulence (Barthlott and Hoose, 2015). The two-moment cloud microphysics scheme of Seifert and Beheng (2006) was used, which uses the super saturation to define a power law, from which CCN concentrations representative of continental conditions are calculated. The droplet size distribution was calculated from the model diagnosed cloud liquid water content and droplet number concentration in every grid box, assuming a modified gamma distribution, with parameters defined in Seifert and Beheng (2006), for droplets in the size range 1 to  $535 \mu\text{m}$ . Figure 1 shows the spatial and temporal mean cloud droplet size distribution for each case investigated. These cases are described in detail in the next section.

Recent work has made significant progress in the development of detailed parameterisations for deposition nucleation, immersion freezing, and contact freezing (Niemand et al., 2012; Tobo et al., 2013; DeMott et al., 2010, 2014; Hiranuma et al., 2014; Steinke et al., 2014; Diehl and Mitra, 2015; Ullrich et al., 2017; Hande et al., 2017). These parameterisations were developed either from observations or theory, and are representative of nucleation on a variety of aerosol species.

In this study, the Steinke et al. (2014) parameterisation for deposition nucleation on Arizona test dust (ATD) was used. This parameterisation is a function of super saturation with respect to ice, and temperature, and is active from 226–250 K. Niemand et al. (2012) was employed to describe immersion freezing, which depends on temperature, and acts between 237–261 K. In these two parameterisations, particle surface area also plays a role through the use of the ice nucleation active surface site (INAS) densities. Comparing these two parameterisations to recently developed formulations by Ullrich et al. (2017) shows good agreement for immersion freezing, and lower nucleation efficiency for desert dust compared to ATD. This provides some measure of confidence in the reliability of the parameterisations used here.

Hande et al. (2017) was used for contact freezing with generic dust aerosols. This parameterisation is a function of aerosol and droplet size and number concentration, relative humidity, temperature, and electrical charges, and is active between 240–268 K. Finally, theoretical expressions of the homogeneous nucleation rate by Jeffery and Austin (1997) were used to describe homogeneous freezing.

A two mode log-normal dust aerosol size distribution was used, as shown in Figure 1, covering particle sizes from 0.1 to  $100 \mu\text{m}$ , which is based on observations from Jungfraujoch research station (Niemand, 2015) (Mode 1:  $N = 0.015 \times 10^6 \text{ m}^{-3}$ ,  $\mu = 1.355 \times 10^{-6} \text{ m}$ ,  $\sigma = 1.443$ , mode 2:  $N = 0.00001 \times 10^6 \text{ m}^{-3}$ ,  $\mu = 8.518 \times 10^{-6} \text{ m}$ ,  $\sigma = 1.358$ ). The dust aerosol concentrations are constant in the vertical dimension, and are not removed by precipitation in the model.



Hande et al. (2015) show that the 5<sup>th</sup> and 95<sup>th</sup> percentiles of dust number concentrations are representative of low and high dust concentrations. These concentrations are often more than an order of magnitude smaller and larger than the median, depending on the season. The dust aerosol properties used in this study correspond roughly to the properties during summer from Hande et al. (2015), during which concentrations and aerosol sizes are the lowest throughout the year. In order to investigate the sensitivity of ice nucleation to the aerosol size distribution, two additional aerosol size distributions are defined in Figure 1, shown as the dashed lines. Here, the total number concentration of both modes was modified by a factor of  $\pm 10$ , which simulates high and low dust aerosol number concentrations.

The aerosol and droplet distributions were divided into 10 bins, over which the integration for the parameterisations was performed. The immersion and contact freezing parameterisations are only applied to cloud droplets. Contact freezing of rain droplets is not considered, since rain drops collect many particles through collision–coalescence and are therefore efficient in the immersion mode (Paukert et al., 2017).

Immersion freezing acts only on the immersed dust aerosols, and contact freezing acts on the interstitial aerosols. The segregation of immersed and interstitial aerosols is treated simplistically in this work, where the ratio of these quantities is pre–defined. In these simulations, 50% of the dust aerosol is defined to be interstitial and hence available for contact freezing, and the remaining 50% is defined to be immersed and available for immersion freezing. This is not necessarily a realistic assumption, however it allows the relative concentrations of immersion and contact INPs to be compared independent of this assumption. Finally, depletion of immersed aerosols is not taken into account in these simulations.

## 2.1 Case study description

Ice nucleation is influenced by ambient environmental conditions, so in order to systematically study the relative contribution of each mode, a distinction between cloud types must be made. In this section, the model configurations for two cases of convection, an idealised orographic cloud, and finally a stratiform cloud, are described.

Since deep convective clouds span temperature ranges relevant for warm and cold cloud microphysics, including into the homogeneous nucleation regime, two cases will be investigated here: an fully idealised warm bubble case, and a semi–idealised cloud. Starting with the former, the thermodynamic profile described in Weisman and Klemp (1982) was used to initialise the simulation, shown in the left panel of Figure 2 as the black lines. A 3D temperature disturbance of 1.5 K, with radius of 10 km, was placed in the centre of the domain at a height of 1.4 km. 100 vertical levels, with  $600 \times 600$  grid cells horizontally, were used, and the time step was 1 second for the duration of the 4 hour simulation.

The semi–idealised deep convective cloud represents a more realistic simulation of convection, and provides an interesting comparison with the previous idealised heat bubble. A detailed description of the model configuration for this case appears in Hande et al. (2017), and is summarised here. A real sounding with CAPE of  $2801 \text{ J kg}^{-1}$  was used to initialise the simulation, and realistic topography was specified at each grid point, as shown in Figure 6 of Hande et al. (2017). The topography represents the region near Jülich, in western Germany, with mountains reaching up to 560 m in the south west of the domain. 100 vertical levels were used, and  $600 \times 600$  grid cells horizontally, with a time step of 2 seconds for the duration of the 9 hour simulation.



To initialise the orographic cloud case, an idealised bell-shaped hill was used along with a real sounding, shown in the right panel of Figure 2 as the black lines. The hill has a maximum height of 800 m and a half-width of 15 km. In the longitudinal direction, 1441 grid points were used, and 271 in the latitudinal direction, with 100 vertical levels. A time step of 1 second was used for the duration of the 4 hour simulation.

5 The final case to be investigated is a stratiform cloud, which was initialised from a real sounding from central Germany during winter, shown in the right panel of Figure 2 as the blue lines. A smaller domain with  $400 \times 400$  horizontal grid points were used, again with 100 vertical levels. In this case, the horizontal wind speed was artificially increased by a factor of 1.5 in the lowest 5.5 km, in order to increase the dynamical forcing enough to activate cloud droplets through shear driven turbulence in the boundary layer. Due to the higher wind speeds in this simulation, a shorter time step of 0.5 seconds was used for the x  
10 hour simulation. All investigated cases employed fully periodic boundary conditions.

### 2.1.1 Spatial distribution of INPs

In this section the spatial distribution of INPs in each mode will be analysed, along with the cloud droplet properties. Contact freezing INPs are parameterised in terms of a rate, so multiplying by the time step of the simulation the number concentrations are obtained. All diagrams in this section are domain mean horizontal cross sections taken at a particular time step indicated in  
15 the figure captions, where the mean is taken over all latitudes. As described in the Section 2, cloud droplet size was calculated from cloud liquid water content and number concentration, assuming a gamma distribution at each grid point. The mode in the cloud droplet radius distribution which is shown in the following diagrams is simply the radius at which the maximum in the cloud droplet size distribution occurred, and the variance and skewness of the distributions are not represented.

Starting with the idealised heat bubble, Figure 3 shows the concentrations of INPs (left panels), along with the cloud droplet  
20 properties (right panels) at 0.5 hrs into the simulation. Immersion and contact freezing both contribute significantly at warmer temperatures, and homogeneous nucleation is a major contributor at colder temperatures. Deposition nucleation, however, is limited to low concentrations occurring over a narrow temperature range.

Looking closer at immersion freezing, there is a trend of higher INP concentrations at colder temperatures. This should be expected since, according to this parameterisation, there is an inverse exponential relationship between INAS density and  
25 temperature.

Contact freezing, on the other hand, shows the opposite trend. Although the contact freezing efficiency also increases exponentially with decreasing temperature, droplet properties have a larger influence on INP concentrations, as discussed in Hande et al. (2017). The highest concentrations in the contact mode occur at around 6 km, co-located with the maximum in cloud droplet size. At colder temperatures above this height, the size and number concentration of cloud droplets is lower, inhibiting  
30 INP formation in this mode.

The final panel in Figure 3 shows the in-cloud relative humidity. On both sides of the central updraft, indicated by the solid contours, there are regions of downdrafts, shown by the dashed contours. This results in lower relative humidity which acts to suppress the formation of INPs.



The results for the semi-idealised deep convective case, shown in Figure 4, are remarkably consistent with the previous case: immersion and contact freezing both dominate, and homogeneous nucleation contributes the most at cold temperatures. Furthermore, the trend in immersion and contact INPs is the same as the idealised heat bubble.

The added complexity in this case highlights an interesting feature of the contact parameterisation employed in this study. Looking at the relative humidity, between about 16–26 km in the horizontal direction, the relative humidity is less than approximately 80 %. Despite this, the concentration of contact INPs are as high as  $10^5 \text{ m}^{-3}$ . That INPs can still form in this environment is a consequence of the phoretic forces (Wang et al., 1978) increasing the collision efficiency between aerosols and cloud droplets in lower humidity regions. Another interesting feature is the high levels of variability in INP concentrations along isotherms. This variability is attributable to the large influence of relative humidity and droplet properties on the contact freezing rate.

The orographic cloud case is shown in Figure 5. Here, homogeneous freezing and deposition nucleation play no role in ice formation, since the cloud top does not reach sufficiently cold temperatures, and immersion INP concentrations are significantly higher than contact. Immersion INP concentrations are more-or-less homogeneously distributed throughout the cloud, and the highest concentrations in the contact mode are co-located with high concentrations of large cloud droplets. In the lee of the hill there is a down draft, indicated by the dashed contours. As was seen in the first case, this reduces the relative humidity and suppresses ice formation.

Given the different dynamical environment of the stratiform case, the resulting INP concentrations, shown in Figure 6, are quite low and the cloud is only sparsely populated with INPs, particularly in the immersion mode. Although the relative humidity in the mid-troposphere is high, around 60–70 %, homogeneous freezing and deposition nucleation do not contribute to ice formation. Immersion INP concentrations are several orders of magnitude larger than contact INP concentrations.

The sounding used to initialise this case, shown in Figure 2, has a strong decrease in moisture at 5.5 km ( $T = 248 \text{ K}$ ,  $p = 475 \text{ hPa}$ ), which inhibits INP formation at colder temperatures. The maximum in the cloud droplet number concentration and size is between 1–2 km, which is outside the temperature range of the contact parameterisation. Therefore, the concentration of contact INPs is reduced due to the lower concentration of smaller cloud droplets in the region of contact freezing.

### 25 3 Temporal evolution of INPs

The temporal development of the ice phase influences a host of cloud properties, including cloud lifetime, radiative properties, and precipitation amount. Figure 7 shows the evolution of each INP mode over the duration of the idealised heat bubble simulation, where the domain mean concentrations over all latitudes and longitudes are taken. INPs in the contact mode appear in low concentrations after 15 min. The cloud develops rapidly, producing high concentrations of INPs in the immersion and contact freezing modes, as well as through homogeneous freezing. Deposition nucleation also plays a role early in the simulation. As the simulation progresses, the initial convective cell dissipates, and after about 2 hours the simulation enters somewhat of a steady state as secondary convection is initiated throughout the domain. Immersion freezing plays less of a role in later stages of the simulation, and all other modes persist with roughly constant concentrations.



The bottom panel show the total precipitation and total water for the duration of the simulation. Since the cloud develops quickly, total water content starts high and diminishes as precipitation develops. Precipitation is initiated after about 1 hour, and there is a break in precipitation coinciding with the dissipation of the main convective cell, with steady precipitation resuming after 2 hours. Interestingly, both cases with higher and lower dust aerosol concentrations result in lower total water and higher precipitation. By the end of the simulation, there is a maximum difference of about 20 % in the total precipitation. The CCN are not influenced by the dust aerosol distribution used in the INP parameterisations.

As in the previous section, the results in the two convective cases are similar, with the temporal evolution of the INPs in the semi-idealised deep convective case closely mirroring the evolution in the idealised heat bubble case, as shown in Figure 8. In the semi-idealised convective case the evolution of the cloud is notably slower, reaching maximum INP concentrations after 4 hours, at which time immersion freezing dominates. Towards the end of the simulation contact freezing becomes more significant. INPs produced at cold temperatures of less than about  $-35\text{ }^{\circ}\text{C}$  reach their maximum late in the simulation, with the greatest contribution from homogeneous freezing.

The total water content for the semi-idealised deep convective case grows steadily for the first half of the simulation. Precipitation is initiated during the peak in ice formation, between 3.5 and 5.5 hours. During this time period is when the immersion and contact INP concentrations reach their maximum, and when homogeneous and deposition nucleation begin to play a role. Perturbations to the dust aerosol concentrations give the opposite effect compared to the previous simulation. That is, both cases of lower and higher dust concentrations give slightly less precipitation.

The temporal evolution of the orographic case, shown in Figure 9, indicates INP production begins in the contact mode soon after initialisation, followed 15 minutes later by the immersion mode. As the simulation progresses, the cloud gets a few hundred metres deeper, immersion INP concentrations get gradually higher and contact INP concentrations get gradually lower.

The total water and total precipitation in the orographic case are much lower than the previous two cases. Here, precipitation begins after 0.5 hours and is light and steady for the duration of the simulation. In contrast to the previous cases, the changes in the aerosol concentrations give a systematic change in total water and total precipitation, where higher aerosol concentrations result in lower total water and higher precipitation, and vice versa. The difference in total precipitation at the end of the simulation is around  $\pm 10\%$ .

The initial development of the stratiform cloud is similar to that of the other cases, where contact INPs are produced first, followed by immersion mode INPs. The contact mode develops slowly over the whole simulation, and is limited to low concentrations. Immersion INPs are produced later, but with higher average concentrations, and the cloud is stable for the duration of the simulation.

While the stratiform case has moderate amounts of liquid water, the total precipitation is the lowest amongst all the cases, so much so that the precipitating liquid doesn't decrease the total water. The simulation with higher aerosol concentrations shows slightly lower total water, but about 25 % more precipitation, whereas the simulation with lower aerosol concentrations has a negligible impact.



#### 4 Discussion

The results thus far are strikingly consistent: immersion and contact freezing dominate at varying times in the simulations, and in the convective cases, homogeneous freezing dominates in the cirrus regime. To quantify this further, Table 1 shows the spatial and temporal mean INP concentrations in each mode, including homogeneous freezing, along with the relative contribution to the total INP concentrations. The aerosol sensitivity simulation for each case are also shown, with - (+) indicating lower (higher) dust aerosol concentrations. The concentrations quoted here are domain wide averages, meaning non-cloudy grid points are included, in order to not bias the results towards short lived, high INP concentrations.

This confirms that immersion freezing is clearly the dominant INP production mechanism in all cases. Contact freezing plays a significant role in most simulations, accounting for up to 1/3 of the total INP concentration in the simulation with normal aerosol concentrations. In the convective cases, homogeneous freezing contributes most at cirrus temperatures, and deposition nucleation plays little role.

The INAS density for immersion freezing depends inverse exponentially on temperature. At temperatures of around 248 K, in the middle of the temperature range for the Niemand et al. (2012) parameterisation, the INAS density approaches  $10^{10} \text{ m}^{-2}$ . This should give an activated fraction of around 0.1 (0.95) for dust aerosols with radius 1 (5)  $\mu\text{m}$ . Given that most dust aerosols are much larger than 1  $\mu\text{m}$ , immersion freezing is efficient in these simulations.

According to Hande et al. (2017), the contact freezing parameterisation depends primarily on aerosol and droplet sizes. These authors show that the highest contact freezing rates are obtained when large aerosol particles ( $\gtrsim 0.3 \mu\text{m}$ ) interact with large cloud droplets ( $\gtrsim 30 \mu\text{m}$ ). Only at the very largest sizes is the frozen fraction one. In these simulations, droplets are mostly smaller than 20  $\mu\text{m}$ , resulting in a contact nucleation rate orders of magnitudes smaller than the maximum possible.

Deposition nucleation as parameterised by Steinke et al. (2014) depends inverse exponentially on temperature and exponentially on ice supersaturation. However it is tightly constrained by observations, such that it is only active at ice supersaturated conditions within a 24 K temperature window. This strongly limits the number of deposition INPs produced in the simulations. The homogeneous freezing parameterisation, on the other hand, is not as tightly constrained, and therefore dominates INP production at cold temperatures.

The effect of perturbations in the dust aerosol concentrations is complex, and depends on the cloud type. In the convective cases, increasing aerosol concentrations increases the relative contribution of immersion freezing by an almost equivalent amount. The other freezing modes then compensate, resulting in a decrease in their relative contribution. The opposite is also true. Decreasing concentrations of dust aerosol decreases the contribution of immersion freezing, while increasing the relative contribution of the other modes. Indeed, in the idealised heat bubble case, contact freezing becomes the dominant mode in low aerosol conditions. There are, however, two exceptions where complex non-monotonic responses are evident: in deposition nucleation in the deep convective simulation, and in contact freezing in the stratiform case.

A natural question arises as to the sensitivity to the thermodynamic profile used to initialise the simulations, and hence how generalisable the results are. Given that the two convective cases, which had vastly different thermodynamic profiles, produced very similar results, this suggests the relative contribution of the ice nucleation modes is more-or-less insensitive to the initial



conditions in these cases. Notice that the droplet properties of both convective cases, shown in Figures 1, 3, and 4, are very similar. Fan et al. (2017), however, show that thermodynamics contributes significantly to cloud microphysical processes for an orographic mixed-phase case. This suggests the sensitivity for non-convectively forced clouds could be larger.

The stratiform case study represents the only cloud type in this study which is weakly forced. Despite high levels of moisture above the main inversion, the conditions for homogeneous freezing or deposition nucleation were not met in this simulation. There is a fundamental difference between cirrus produced in different dynamical environments. In the convective cases, liquid water is lifted from the mixed-phase regime to colder temperatures, where it freezes. Since the stratiform case is weakly forced, the origin of the moisture is from higher altitudes. These two categories are known as either 'liquid origin cirrus' or 'in-situ cirrus' (Krämer et al., 2016; Luebke et al., 2016). Since the stratiform cloud investigated here has no cirrus, the dominant ice forming mechanism for this so-called 'in-situ cirrus' remains an open question.

A few of the assumptions built into the simulations may influence the results presented. The even separation of immersed and interstitial aerosols will most likely cause an overestimate of contact freezing, in particular in the updraft where the super saturation is the highest, and immersion freezing could be more dominant. Neglecting contact freezing of rain droplets should not have a large influence on the dominant freezing mode in these simulations, however it could affect the precipitation formation (Paukert et al. (2017)). A final consideration concerning the aerosol species needs to be made. Aerosol composition has a large influence on nucleation ability in different temperature and super saturation regimes. Whether this has a significant impact on the dominant ice nucleation mode remains to be investigated.

## 5 Conclusions

A number of high resolution modelling case studies are presented in order to systematically investigate which ice nucleation modes dominate for a number of typical cloud types. The results indicate that immersion freezing dominates in all cases. Contact nucleation plays a significant role in most simulations, accounting for between about 2–33 % of total INP concentrations under the reference aerosol conditions. Deposition nucleation only contributes a fraction of a percent in the convective cases, and homogeneous freezing accounts for up to 6 % of total INP concentrations. However in the non-convective cases, no INPs were produced in the cirrus regime.

In the later stages of the convective clouds, homogeneous freezing became more important, and contact freezing dominated at warm temperatures. The orographic and stratiform case reached a steady state soon after the formation of the cloud. The occurrence of precipitation is not correlated with any one ice nucleation mode, instead occurs at the same time as multiple ice nucleation modes, including homogeneous nucleation.

Since the results from the two convective cases were quite similar, this suggests ice nucleation could be insensitive to thermodynamical conditions in these cases. The main consequence of the much higher CAPE in the heat bubble case, compared to the semi-idealised deep convective case, was faster cloud development.

For the convective cases, perturbation in aerosol concentrations produced proportional changes in the relative contribution of immersion freezing INPs. The relative contribution of the other modes decreased. The opposite occurred for the orographic



case, where the relative contribution of contact increased under higher aerosol concentrations, and immersion decreased. In the stratiform case, all aerosol perturbations produced relatively more immersion freezing INPs, and fewer contact INPs. This indicates aerosol conditions have a complex influence of the dominant ice nucleation mode.

*Data availability.* The data is available from the corresponding author upon request.

5 *Competing interests.* No competing interests are present.

*Acknowledgements.* This work was funded by the Deutsche Forschungsgesellschaft through the research unit INUIT-2 (FOR 1525, HO4612/1-2). The authors would like to gratefully acknowledge Christian Barthlott (KIT) and Lulin Xue (NCAR) for assistance with the model configuration.



## References

- Ansmann, A., Tesche, M., Seifert, P., Althausen, D., Engelmann, R., Fruntke, J., Wandinger, U., Mattis, I., and Müller, D.: Evolution of the ice phase in tropical altocumulus: SAMUM lidar observations over Cape Verde, *Journal of Geophysical Research: Atmospheres* (1984–2012), 114, 2009.
- 5 Barthlott, C. and Hoose, C.: Spatial and temporal variability of clouds and precipitation over Germany: multiscale simulations across the "gray zone", *Atmospheric Chemistry & Physics*, 15, 12 361–12 384, 2015.
- Carro-Calvo, L., Hoose, C., Stengel, M., and Salcedo-Sanz, S.: Cloud Glaciation Temperature Estimation from Passive Remote Sensing Data with Evolutionary Computing, *Journal of Geophysical Research: Atmospheres*, 2016.
- Cui, Z., Carslaw, K. S., Yin, Y., and Davies, S.: A numerical study of aerosol effects on the dynamics and microphysics of a deep convective  
10 cloud in a continental environment, *Journal of Geophysical Research: Atmospheres*, 111, 2006.
- Cziczo, D. J., Ladino, L., Boose, Y., Kanji, Z. A., Kupiszewski, P., Lance, S., Mertes, S., and Wex, H.: Chapter 8: Measurements of Ice Nucleating Particles and Ice Residuals, *Meteorological Monographs*, 58, 2016.
- De Boer, G., Morrison, H., Shupe, M., and Hildner, R.: Evidence of liquid dependent ice nucleation in high-latitude stratiform clouds from surface remote sensors, *Geophysical Research Letters*, 38, 2011.
- 15 DeMott, P., Prenni, A., Liu, X., Kreidenweis, S., Petters, M., Twohy, C., Richardson, M., Eidhammer, T., and Rogers, D.: Predicting global atmospheric ice nuclei distributions and their impacts on climate, *Proceedings of the National Academy of Sciences*, 107, 11 217–11 222, 2010.
- DeMott, P., Prenni, A., McMeeking, G., Sullivan, R., Petters, M., Tobo, Y., Niemand, M., Möhler, O., Snider, J., Wang, Z., and Kreidenweis, S.: Integrating laboratory and field data to quantify the immersion freezing ice nucleation activity of mineral dust particles, *Atmospheric  
20 Chemistry and Physics*, 14, 17 359–17 400, 2014.
- Diehl, K. and Mitra, S.: New particle-dependent parameterizations of heterogeneous freezing processes: sensitivity studies of convective clouds with an air parcel model., *Atmospheric Chemistry & Physics Discussions*, 15, 2015.
- Durant, A. J. and Shaw, R. A.: Evaporation freezing by contact nucleation inside-out, *Geophysical Research Letters*, 32, 2005.
- Fan, J., Ruby Leung, L., Rosenfeld, D., and DeMott, P. J.: Effects of cloud condensation nuclei and ice nucleating particles on precipitation  
25 processes and supercooled liquid in mixed-phase orographic clouds, *Atmos. Chem. Phys.*, 1680, 7324, 2017.
- Field, P., Heymsfield, A., Shipway, B., DeMott, P., Pratt, K., Rogers, D., Stith, J., and Prather, K.: Ice in clouds experiment-layer clouds. Part II: Testing characteristics of heterogeneous ice formation in lee wave clouds, *Journal of the Atmospheric Sciences*, 69, 1066–1079, 2012.
- Hande, L., Engler, C., Hoose, C., and Tegen, I.: Seasonal variability of Saharan desert dust and ice nucleating particles over Europe, *Atmospheric Chemistry and Physics*, 15, 4389–4397, 2015.
- 30 Hande, L., Hoose, C., and Barthlott, C.: Aerosol and droplet dependent contact freezing: Parameterisation development and case study, Accepted: *Journal of Atmospheric Sciences*, 2017.
- Hiranuma, N., Paukert, M., Steinke, I., Zhang, K., Kulkarni, G., Hoose, C., Schnaiter, M., Saathoff, H., and Möhler, O.: A comprehensive parameterization of heterogeneous ice nucleation of dust surrogate: laboratory study with hematite particles and its application to atmospheric models, *Atmospheric Chemistry and Physics Discussions*, 14, 16 493–16 528, 2014.
- 35 Hoose, C. and Möhler, O.: Heterogeneous ice nucleation on atmospheric aerosols: a review of results from laboratory experiments, *Atmospheric Chemistry and Physics*, 12, 9817–9854, 2012.



- Hoose, C., Kristjánsson, J. E., Chen, J.-P., and Hazra, A.: A classical-theory-based parameterization of heterogeneous ice nucleation by mineral dust, soot, and biological particles in a global climate model, *Journal of the Atmospheric Sciences*, 67, 2483–2503, 2010.
- Jeffery, C. and Austin, P.: Homogeneous nucleation of supercooled water: Results from a new equation of state, *JOURNAL OF GEOPHYSICAL RESEARCH-ALL SERIES-*, 102, 25–269, 1997.
- 5 Koop, T. and Murray, B. J.: A physically constrained classical description of the homogeneous nucleation of ice in water, *The Journal of Chemical Physics*, 145, 211 915, 2016.
- Krämer, M., Rolf, C., Luebke, A., Afchine, A., Spelten, N., Costa, A., Meyer, J., Zöger, M., Smith, J., Herman, R. L., Buchholz, B., Ebert, V., Baumgardner, D., Borrmann, S., Klingebiel, M., and Avallone, L.: A microphysics guide to cirrus clouds-Part 1: Cirrus types, *Atmospheric Chemistry and Physics*, 16, 3463, 2016.
- 10 Ladino, L., Stetzer, O., and Lohmann, U.: Contact freezing: a review of experimental studies, *Atmospheric Chemistry and Physics*, 13, 9745–9769, 2013.
- Luebke, A. E., Afchine, A., Costa, A., Groß, J.-U., Meyer, J., Rolf, C., Spelten, N., Avallone, L. M., Baumgardner, D., and Krämer, M.: The origin of midlatitude ice clouds and the resulting influence on their microphysical properties, *Atmospheric Chemistry and Physics*, 16, 5793–5809, 2016.
- 15 Murray, B., O’Sullivan, D., Atkinson, J., and Webb, M.: Ice nucleation by particles immersed in supercooled cloud droplets, *Chemical Society Reviews*, 41, 6519–6554, 2012.
- Nagare, B., Marcolli, C., Welti, A., Stetzer, O., and Lohmann, U.: Comparing contact and immersion freezing from continuous flow diffusion chambers, *Atmospheric Chemistry Physics*, 16, 2016.
- Niemand, M.: Dust Size Distribution, Personal Communication, 2015.
- 20 Niemand, M., Möhler, O., Vogel, B., Vogel, H., Hoose, C., Connolly, P., Klein, H., Bingemer, H., DeMott, P., Skrotzki, J., et al.: A particle-surface-area-based parameterization of immersion freezing on desert dust particles, *Journal of the Atmospheric Sciences*, 69, 3077–3092, 2012.
- Paukert, M., Hoose, C., and Simmel, M.: Redistribution of ice nuclei between cloud and rain droplets: Parameterization and application to deep convective clouds, *Journal of Advances in Modeling Earth Systems*, 2017.
- 25 Philips, V. T., Donner, L. J., and Garner, S. T.: Nucleation processes in deep convection simulated by a cloud-system-resolving model with double-moment bulk microphysics, *Journal of the atmospheric sciences*, 64, 738–761, 2007.
- Rogers, D. C., DeMott, P. J., Kreidenweis, S. M., and Chen, Y.: Measurements of ice nucleating aerosols during SUCCESS, *Geophysical research letters*, 25, 1383–1386, 1998.
- Schättler, U., Doms, G., and Schraff, C.: A description of the nonhydrostatic regional COSMO-model. Part vii: user’s guide, *Deutscher Wetterdienst Rep. COSMO-Model*, 4, 142, 2008.
- 30 Seifert, A. and Beheng, K.: A two-moment cloud microphysics parameterization for mixed-phase clouds. Part 1: Model description, *Meteorology and atmospheric physics*, 92, 45–66, 2006.
- Steinke, I., Hoose, C., Möhler, O., Connolly, P., and Leisner, T.: A new temperature and humidity dependent surface site density approach for deposition ice nucleation, *Atmospheric Chemistry and Physics Discussions*, 14, 18 499–18 539, 2014.
- 35 Tobo, Y., Prenni, A. J., DeMott, P. J., Huffman, J. A., McCluskey, C. S., Tian, G., Pöhlker, C., Pöschl, U., and Kreidenweis, S. M.: Biological aerosol particles as a key determinant of ice nuclei populations in a forest ecosystem, *Journal of Geophysical Research: Atmospheres*, 118, 2013.



- Ullrich, R., Hoose, C., Möhler, O., Niemand, M., Wagner, R., Höhler, K., Hiranuma, N., Saathoff, H., and Leisner, T.: A new ice nucleation active site parameterization for desert dust and soot, *Journal of the Atmospheric Sciences*, 74, 699–717, 2017.
- Vali, G., DeMott, P., Möhler, O., and Whale, T.: Technical Note: A proposal for ice nucleation terminology, *Atmospheric Chemistry and Physics*, 15, 10 263–10 270, 2015.
- 5 Wang, P., Grover, S., and Pruppacher, H.: On the effect of electric charges on the scavenging of aerosol particles by clouds and small raindrops, *Journal of the Atmospheric Sciences*, 35, 1735–1743, 1978.
- Weisman, M. L. and Klemp, J. B.: The dependence of numerically simulated convective storms on vertical wind shear and buoyancy, *Monthly Weather Review*, 110, 504–520, 1982.
- Westbrook, C. D. and Illingworth, A. J.: Evidence that ice forms primarily in supercooled liquid clouds at temperatures > -27 C, *Geophysical Research Letters*, 38, 2011.
- 10 Wiacek, A. and Peter, T.: On the availability of uncoated mineral dust ice nuclei in cold cloud regions, *Geophysical Research Letters*, 36, 2009.



## References

- Ansmann, A., Tesche, M., Seifert, P., Althausen, D., Engelmann, R., Fruntke, J., Wandinger, U., Mattis, I., and Müller, D.: Evolution of the ice phase in tropical altocumulus: SAMUM lidar observations over Cape Verde, *Journal of Geophysical Research: Atmospheres* (1984–2012), 114, 2009.
- 5 Barthlott, C. and Hoose, C.: Spatial and temporal variability of clouds and precipitation over Germany: multiscale simulations across the "gray zone", *Atmospheric Chemistry & Physics*, 15, 12 361–12 384, 2015.
- Carro-Calvo, L., Hoose, C., Stengel, M., and Salcedo-Sanz, S.: Cloud Glaciation Temperature Estimation from Passive Remote Sensing Data with Evolutionary Computing, *Journal of Geophysical Research: Atmospheres*, 2016.
- Cui, Z., Carslaw, K. S., Yin, Y., and Davies, S.: A numerical study of aerosol effects on the dynamics and microphysics of a deep convective  
10 cloud in a continental environment, *Journal of Geophysical Research: Atmospheres*, 111, 2006.
- Cziczo, D. J., Ladino, L., Boose, Y., Kanji, Z. A., Kupiszewski, P., Lance, S., Mertes, S., and Wex, H.: Chapter 8: Measurements of Ice Nucleating Particles and Ice Residuals, *Meteorological Monographs*, 58, 2016.
- De Boer, G., Morrison, H., Shupe, M., and Hildner, R.: Evidence of liquid dependent ice nucleation in high-latitude stratiform clouds from surface remote sensors, *Geophysical Research Letters*, 38, 2011.
- 15 DeMott, P., Prenni, A., Liu, X., Kreidenweis, S., Petters, M., Twohy, C., Richardson, M., Eidhammer, T., and Rogers, D.: Predicting global atmospheric ice nuclei distributions and their impacts on climate, *Proceedings of the National Academy of Sciences*, 107, 11 217–11 222, 2010.
- DeMott, P., Prenni, A., McMeeking, G., Sullivan, R., Petters, M., Tobo, Y., Niemand, M., M<sup>o</sup>hler, O., Snider, J., Wang, Z., and Kreidenweis, S.: Integrating laboratory and field data to quantify the immersion freezing ice nucleation activity of mineral dust particles, *Atmospheric  
20 Chemistry and Physics*, 14, 17 359–17 400, 2014.
- Diehl, K. and Mitra, S.: New particle-dependent parameterizations of heterogeneous freezing processes: sensitivity studies of convective clouds with an air parcel model., *Atmospheric Chemistry & Physics Discussions*, 15, 2015.
- Durant, A. J. and Shaw, R. A.: Evaporation freezing by contact nucleation inside-out, *Geophysical Research Letters*, 32, 2005.
- Fan, J., Ruby Leung, L., Rosenfeld, D., and DeMott, P. J.: Effects of cloud condensation nuclei and ice nucleating particles on precipitation  
25 processes and supercooled liquid in mixed-phase orographic clouds, *Atmos. Chem. Phys.*, 1680, 7324, 2017.
- Field, P., Heymsfield, A., Shipway, B., DeMott, P., Pratt, K., Rogers, D., Stith, J., and Prather, K.: Ice in clouds experiment-layer clouds. Part II: Testing characteristics of heterogeneous ice formation in lee wave clouds, *Journal of the Atmospheric Sciences*, 69, 1066–1079, 2012.
- Hande, L., Engler, C., Hoose, C., and Tegen, I.: Seasonal variability of Saharan desert dust and ice nucleating particles over Europe, *Atmospheric Chemistry and Physics*, 15, 4389–4397, 2015.
- 30 Hande, L., Hoose, C., and Barthlott, C.: Aerosol and droplet dependent contact freezing: Parameterisation development and case study, Accepted: *Journal of Atmospheric Sciences*, 2017.
- Hiranuma, N., Paukert, M., Steinke, I., Zhang, K., Kulkarni, G., Hoose, C., Schnaiter, M., Saathoff, H., and Möhler, O.: A comprehensive parameterization of heterogeneous ice nucleation of dust surrogate: laboratory study with hematite particles and its application to atmospheric models, *Atmospheric Chemistry and Physics Discussions*, 14, 16 493–16 528, 2014.
- 35 Hoose, C. and Möhler, O.: Heterogeneous ice nucleation on atmospheric aerosols: a review of results from laboratory experiments, *Atmospheric Chemistry and Physics*, 12, 9817–9854, 2012.



- Hoose, C., Kristjánsson, J. E., Chen, J.-P., and Hazra, A.: A classical-theory-based parameterization of heterogeneous ice nucleation by mineral dust, soot, and biological particles in a global climate model, *Journal of the Atmospheric Sciences*, 67, 2483–2503, 2010.
- Jeffery, C. and Austin, P.: Homogeneous nucleation of supercooled water: Results from a new equation of state, *JOURNAL OF GEOPHYSICAL RESEARCH-ALL SERIES-*, 102, 25–269, 1997.
- 5 Koop, T. and Murray, B. J.: A physically constrained classical description of the homogeneous nucleation of ice in water, *The Journal of Chemical Physics*, 145, 211 915, 2016.
- Krämer, M., Rolf, C., Luebke, A., Afchine, A., Spelten, N., Costa, A., Meyer, J., Zöger, M., Smith, J., Herman, R. L., Buchholz, B., Ebert, V., Baumgardner, D., Borrmann, S., Klingebiel, M., and Avallone, L.: A microphysics guide to cirrus clouds-Part 1: Cirrus types, *Atmospheric Chemistry and Physics*, 16, 3463, 2016.
- 10 Ladino, L., Stetzer, O., and Lohmann, U.: Contact freezing: a review of experimental studies, *Atmospheric Chemistry and Physics*, 13, 9745–9769, 2013.
- Luebke, A. E., Afchine, A., Costa, A., Groß, J.-U., Meyer, J., Rolf, C., Spelten, N., Avallone, L. M., Baumgardner, D., and Krämer, M.: The origin of midlatitude ice clouds and the resulting influence on their microphysical properties, *Atmospheric Chemistry and Physics*, 16, 5793–5809, 2016.
- 15 Murray, B., O’Sullivan, D., Atkinson, J., and Webb, M.: Ice nucleation by particles immersed in supercooled cloud droplets, *Chemical Society Reviews*, 41, 6519–6554, 2012.
- Nagare, B., Marcolli, C., Welti, A., Stetzer, O., and Lohmann, U.: Comparing contact and immersion freezing from continuous flow diffusion chambers, *Atmospheric Chemistry Physics*, 16, 2016.
- Niemand, M.: Dust Size Distribution, Personal Communication, 2015.
- 20 Niemand, M., Möhler, O., Vogel, B., Vogel, H., Hoose, C., Connolly, P., Klein, H., Bingemer, H., DeMott, P., Skrotzki, J., et al.: A particle-surface-area-based parameterization of immersion freezing on desert dust particles, *Journal of the Atmospheric Sciences*, 69, 3077–3092, 2012.
- Paukert, M., Hoose, C., and Simmel, M.: Redistribution of ice nuclei between cloud and rain droplets: Parameterization and application to deep convective clouds, *Journal of Advances in Modeling Earth Systems*, 2017.
- 25 Philips, V. T., Donner, L. J., and Garner, S. T.: Nucleation processes in deep convection simulated by a cloud-system-resolving model with double-moment bulk microphysics, *Journal of the atmospheric sciences*, 64, 738–761, 2007.
- Rogers, D. C., DeMott, P. J., Kreidenweis, S. M., and Chen, Y.: Measurements of ice nucleating aerosols during SUCCESS, *Geophysical research letters*, 25, 1383–1386, 1998.
- Schättler, U., Doms, G., and Schraff, C.: A description of the nonhydrostatic regional COSMO-model. Part vii: user’s guide, *Deutscher Wetterdienst Rep. COSMO-Model*, 4, 142, 2008.
- 30 Seifert, A. and Beheng, K.: A two-moment cloud microphysics parameterization for mixed-phase clouds. Part 1: Model description, *Meteorology and atmospheric physics*, 92, 45–66, 2006.
- Steinke, I., Hoose, C., Möhler, O., Connolly, P., and Leisner, T.: A new temperature and humidity dependent surface site density approach for deposition ice nucleation, *Atmospheric Chemistry and Physics Discussions*, 14, 18 499–18 539, 2014.
- 35 Tobo, Y., Prenni, A. J., DeMott, P. J., Huffman, J. A., McCluskey, C. S., Tian, G., Pöhlker, C., Pöschl, U., and Kreidenweis, S. M.: Biological aerosol particles as a key determinant of ice nuclei populations in a forest ecosystem, *Journal of Geophysical Research: Atmospheres*, 118, 2013.



- Ullrich, R., Hoose, C., Möhler, O., Niemand, M., Wagner, R., Höhler, K., Hiranuma, N., Saathoff, H., and Leisner, T.: A new ice nucleation active site parameterization for desert dust and soot, *Journal of the Atmospheric Sciences*, 74, 699–717, 2017.
- Vali, G., DeMott, P., Möhler, O., and Whale, T.: Technical Note: A proposal for ice nucleation terminology, *Atmospheric Chemistry and Physics*, 15, 10 263–10 270, 2015.
- 5 Wang, P., Grover, S., and Pruppacher, H.: On the effect of electric charges on the scavenging of aerosol particles by clouds and small raindrops, *Journal of the Atmospheric Sciences*, 35, 1735–1743, 1978.
- Weisman, M. L. and Klemp, J. B.: The dependence of numerically simulated convective storms on vertical wind shear and buoyancy, *Monthly Weather Review*, 110, 504–520, 1982.
- Westbrook, C. D. and Illingworth, A. J.: Evidence that ice forms primarily in supercooled liquid clouds at temperatures > -27 C, *Geophysical*  
10 *Research Letters*, 38, 2011.
- Wiacek, A. and Peter, T.: On the availability of uncoated mineral dust ice nuclei in cold cloud regions, *Geophysical Research Letters*, 36, 2009.

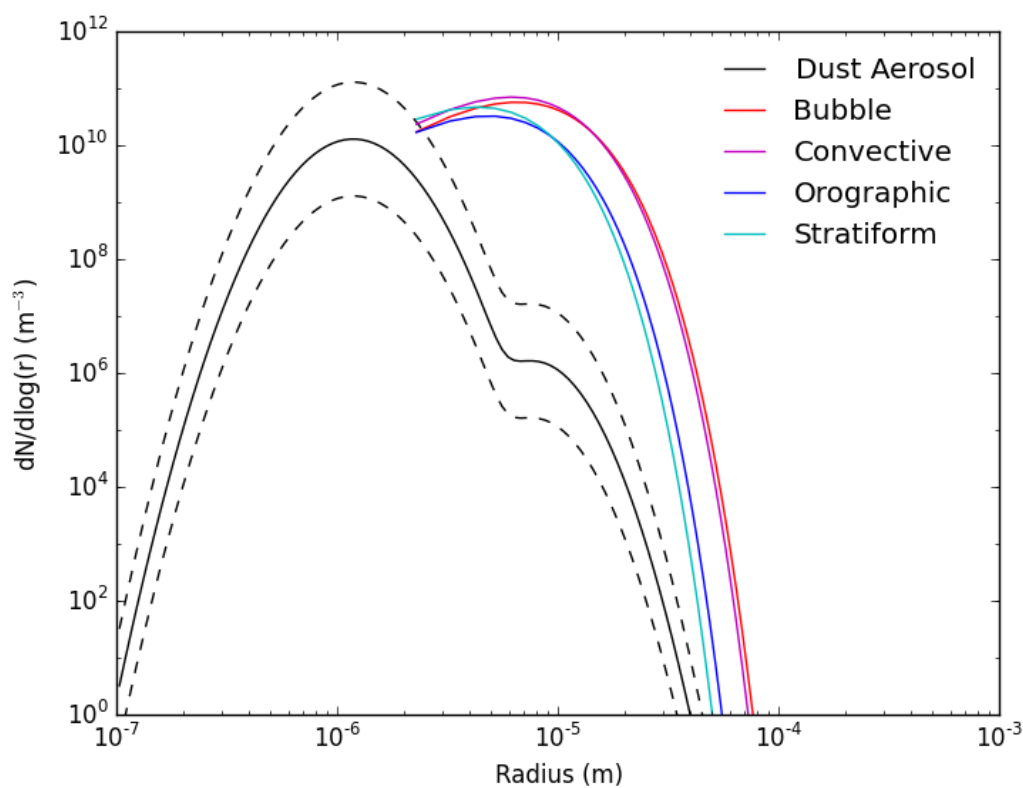


**Figure 1.** Prescribed dust aerosol size distribution, and derived mean cloud droplet size distribution for all cases. Dashed lines indicate dust aerosol size distribution for sensitivity studies.

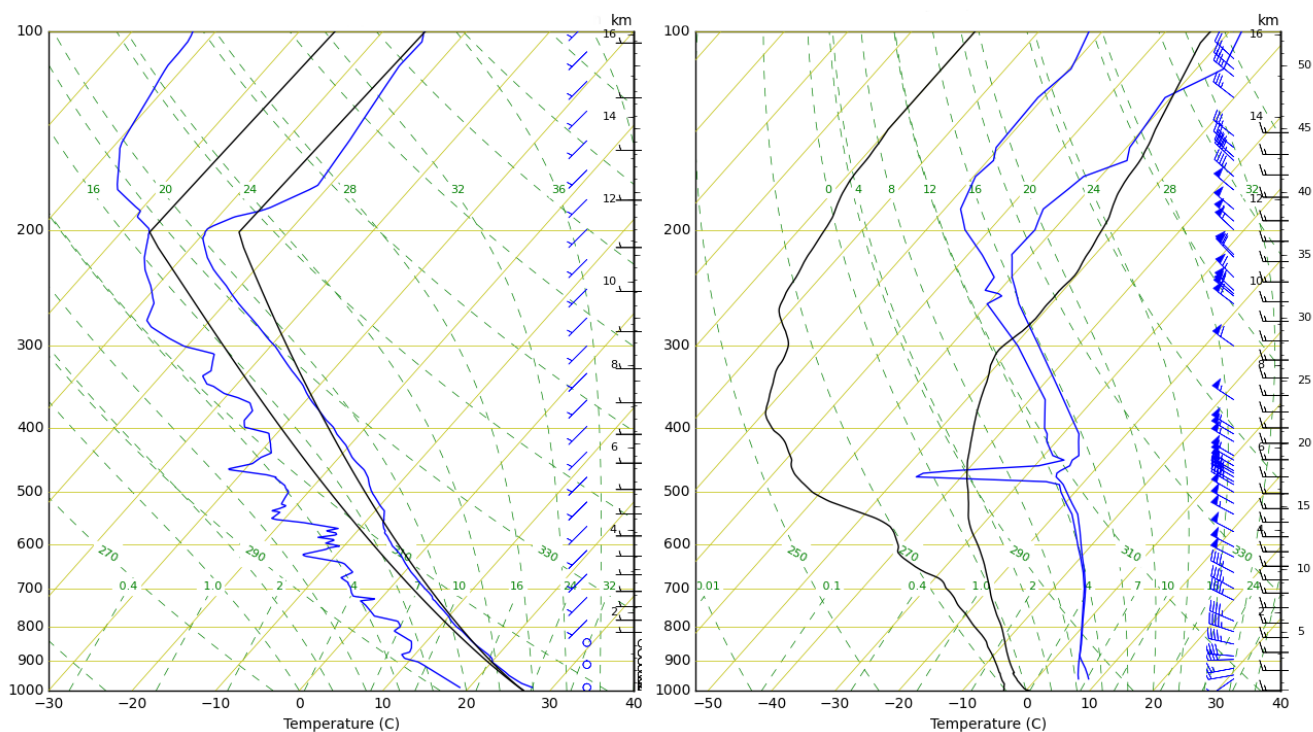


**Figure 2.** Thermodynamic sounding used to initialise the cases. Left panel: idealised heat bubble (black), semi-idealised deep convective (blue). Right panel: orographic (black), stratiform (blue).

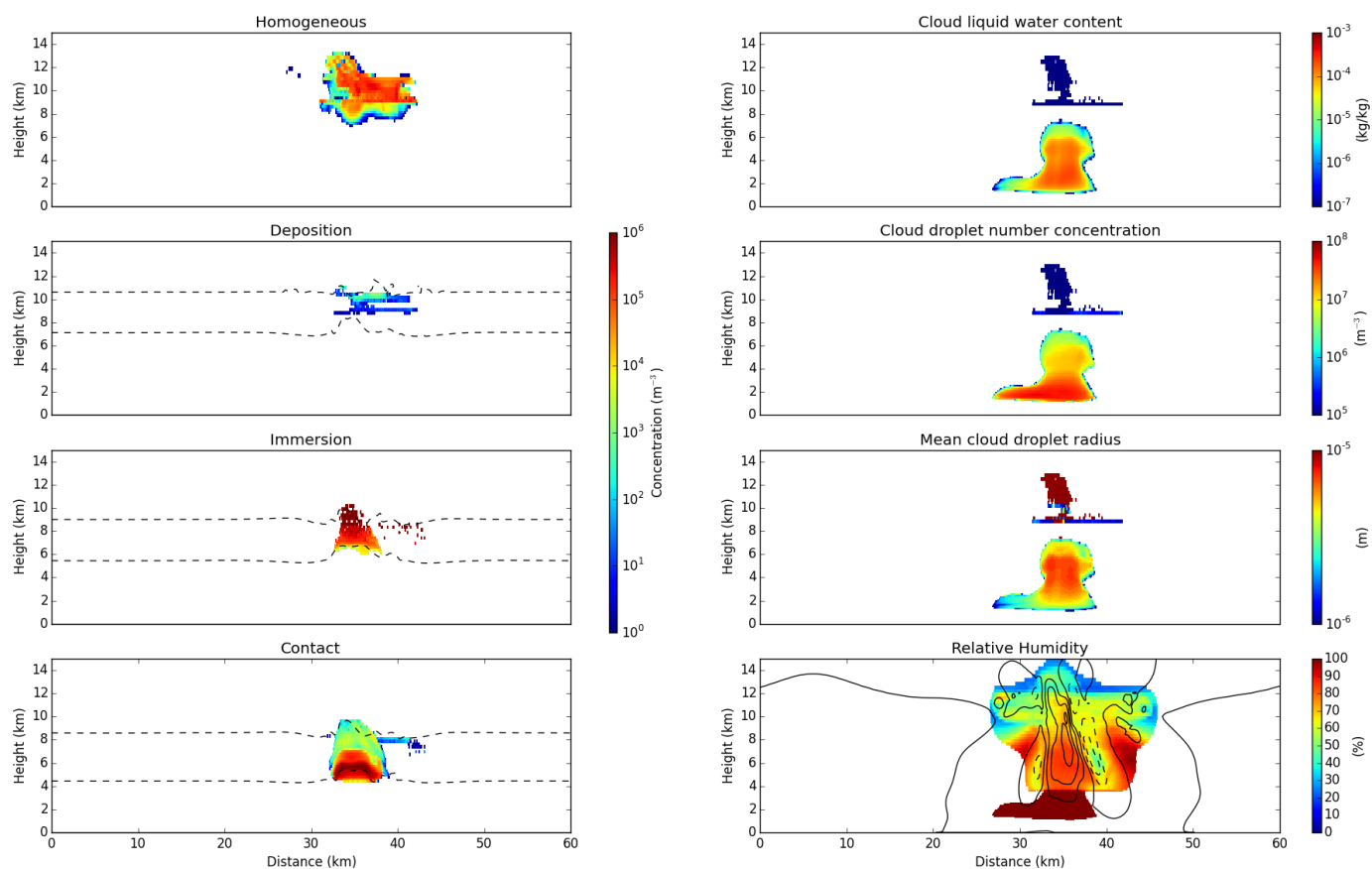


**Figure 3.** Domain mean horizontal cross section of INP number concentrations in each mode (left), cloud droplet properties (right) for the heat bubble convective cloud at 0.5 hrs into the simulation. Dashed horizontal lines represent the temperature limits of the parameterisations. Contours represent the sign of the vertical velocity (solid: positive, dashed: negative).

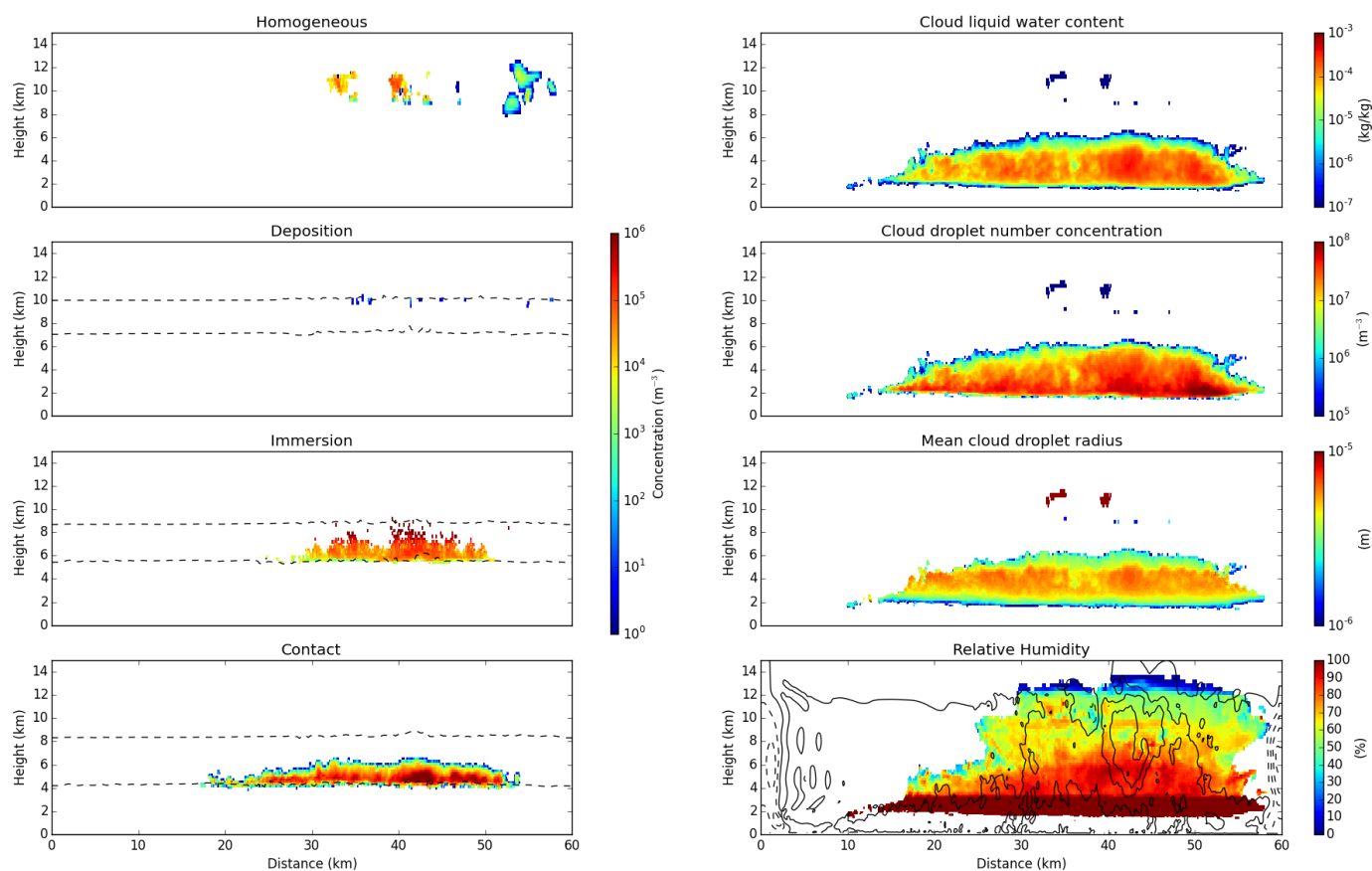


**Figure 4.** Domain mean horizontal cross section of INP number concentrations in each mode (left), cloud droplet properties (right) for the semi-idealised deep convective cloud at 4 hrs into the simulation. Dashed horizontal lines represent the temperature limits of the parameterisations. Contours represent the sign of the vertical velocity (solid: positive, dashed: negative).

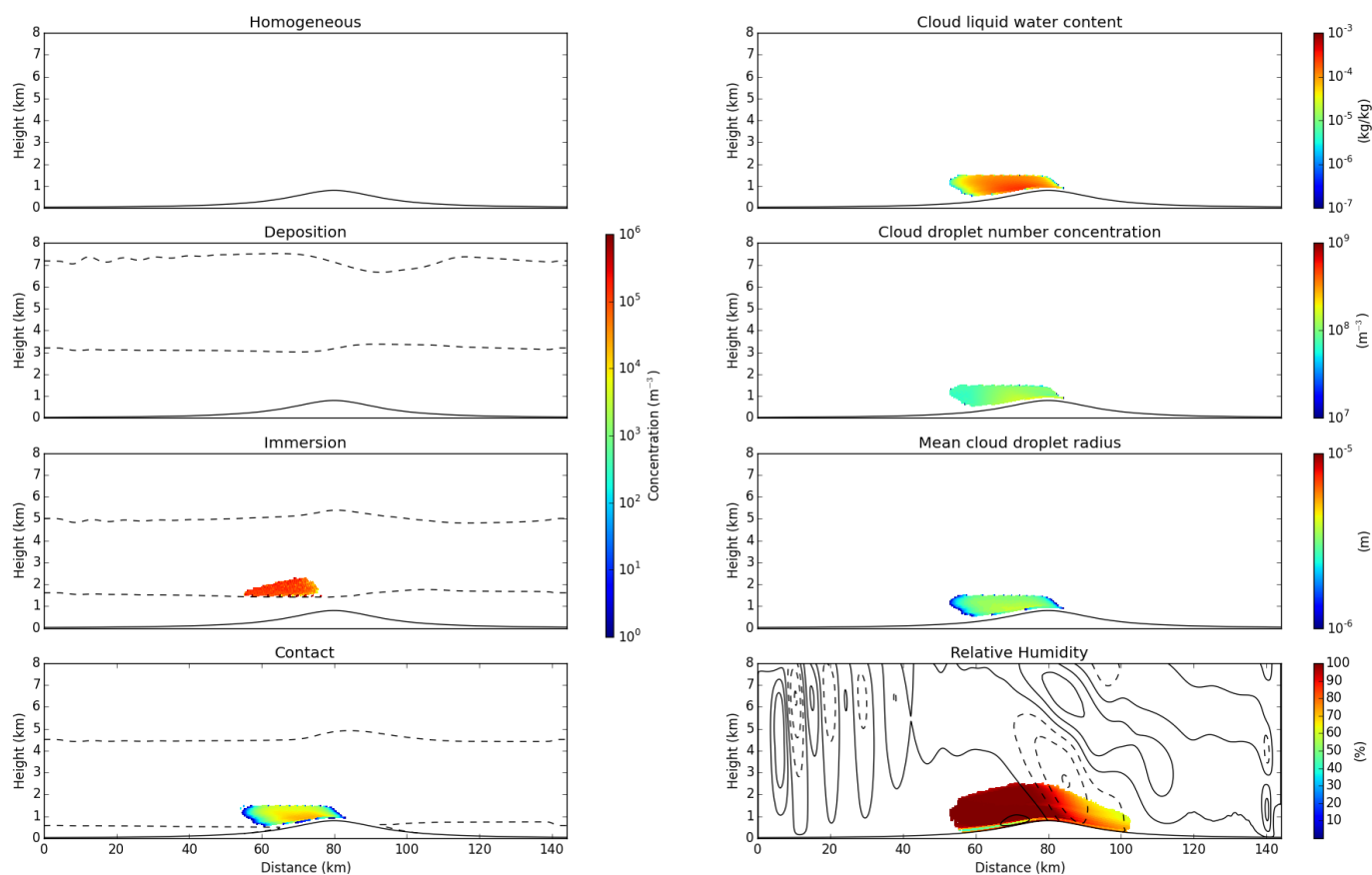


**Figure 5.** Domain mean horizontal cross section of INP number concentrations in each mode (left), cloud droplet properties (right) for the orographic cloud at 2 hrs into the simulation. Dashed horizontal lines represent the temperature limits of the parameterisations. Contours represent the sign of the vertical velocity (solid: positive, dashed: negative).

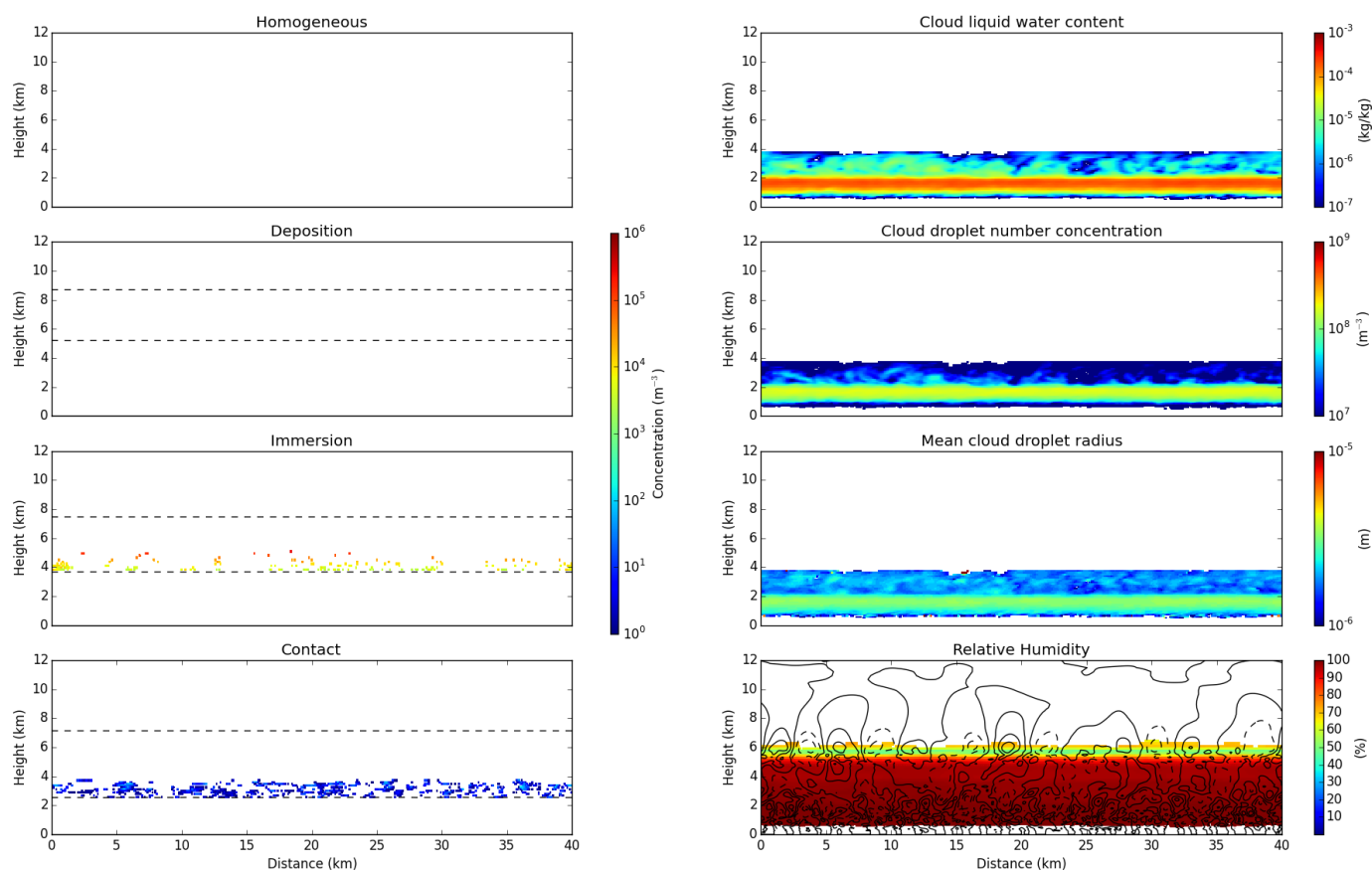


**Figure 6.** Domain mean horizontal cross section of INP number concentrations in each mode (left), cloud droplet properties (right) for the stratiform cloud at 3 hrs into the simulation. Dashed horizontal lines represent the temperature limits of the parameterisations. Contours represent the sign of the vertical velocity (solid: positive, dashed: negative).

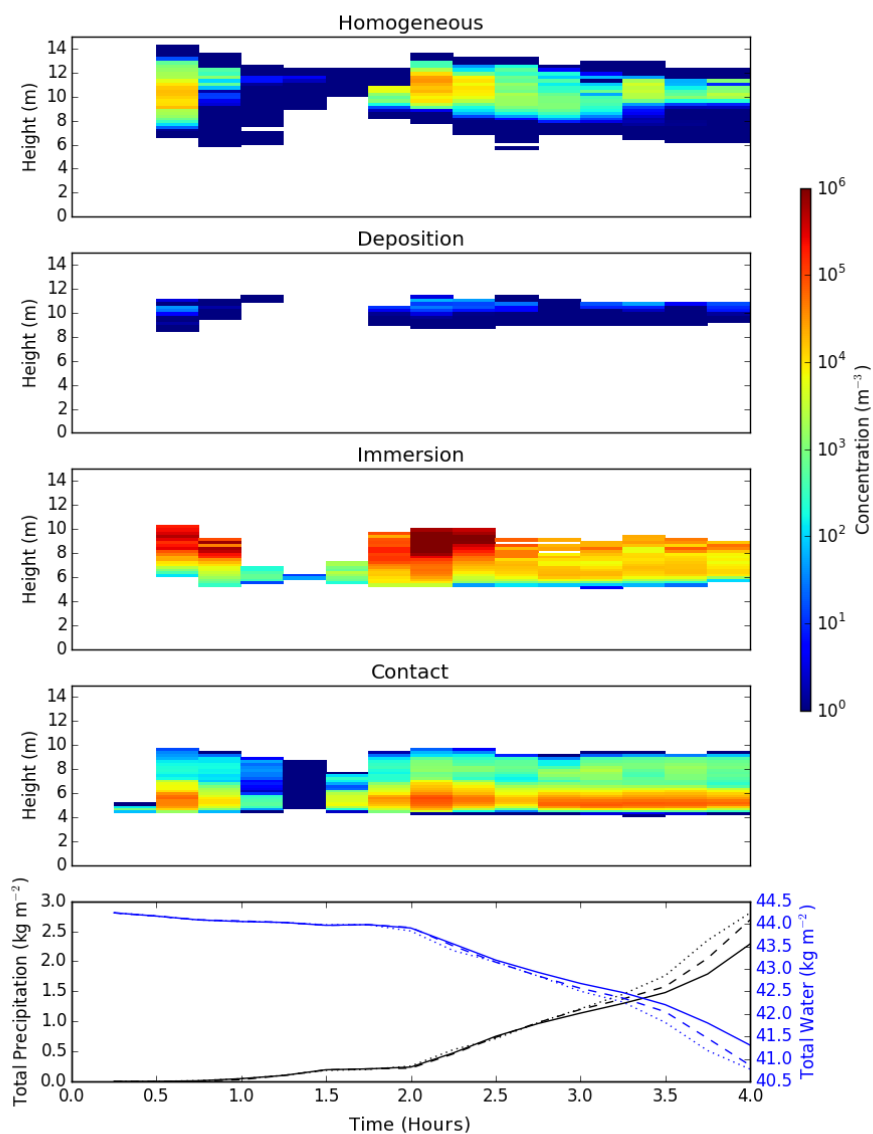


**Figure 7.** Temporal evolution of INP number concentrations in each mode for the heat bubble convective cloud. Bottom panel shows total precipitation (black) and total water (blue). Dashed (dotted) line is for the high (low) aerosol simulation.

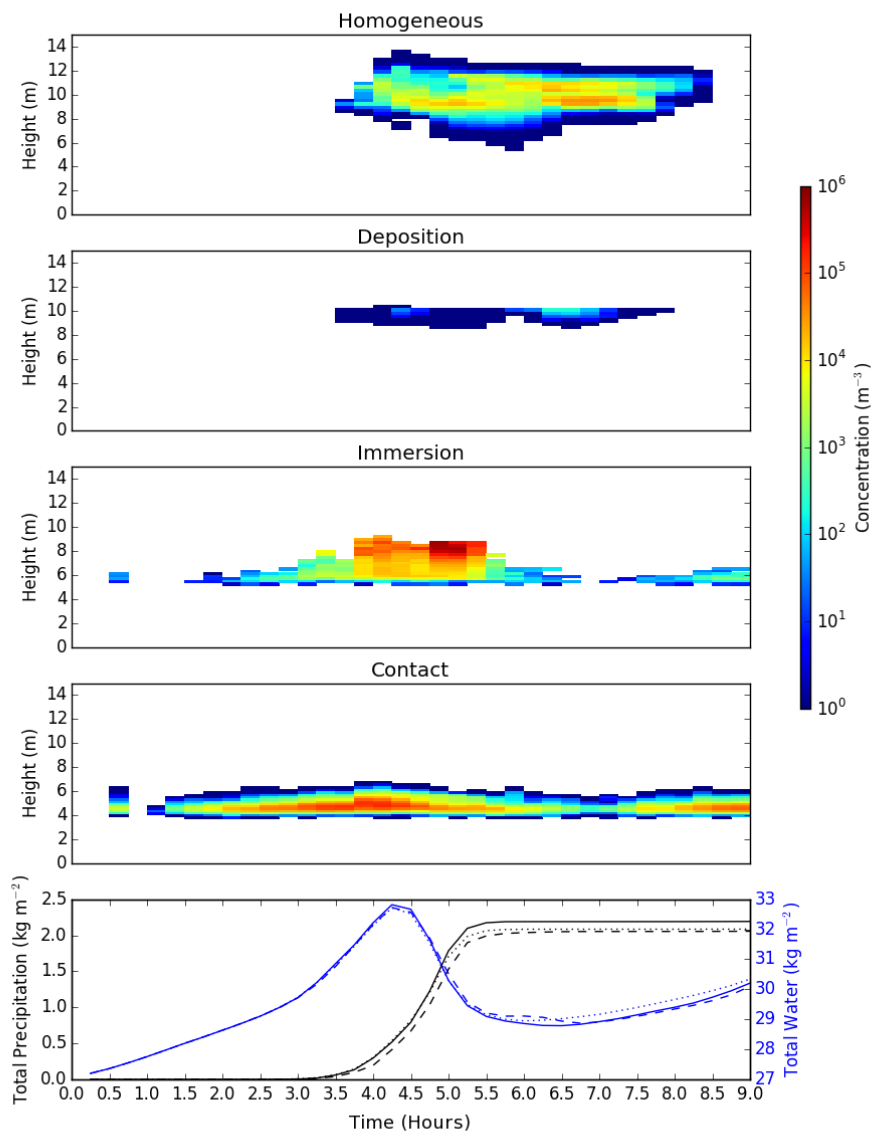


**Figure 8.** Temporal evolution of INP number concentrations in each mode for the semi-idealised deep convective cloud. Bottom panel shows total precipitation (black) and total water (blue). Dashed (dotted) line is for the high (low) aerosol simulation.

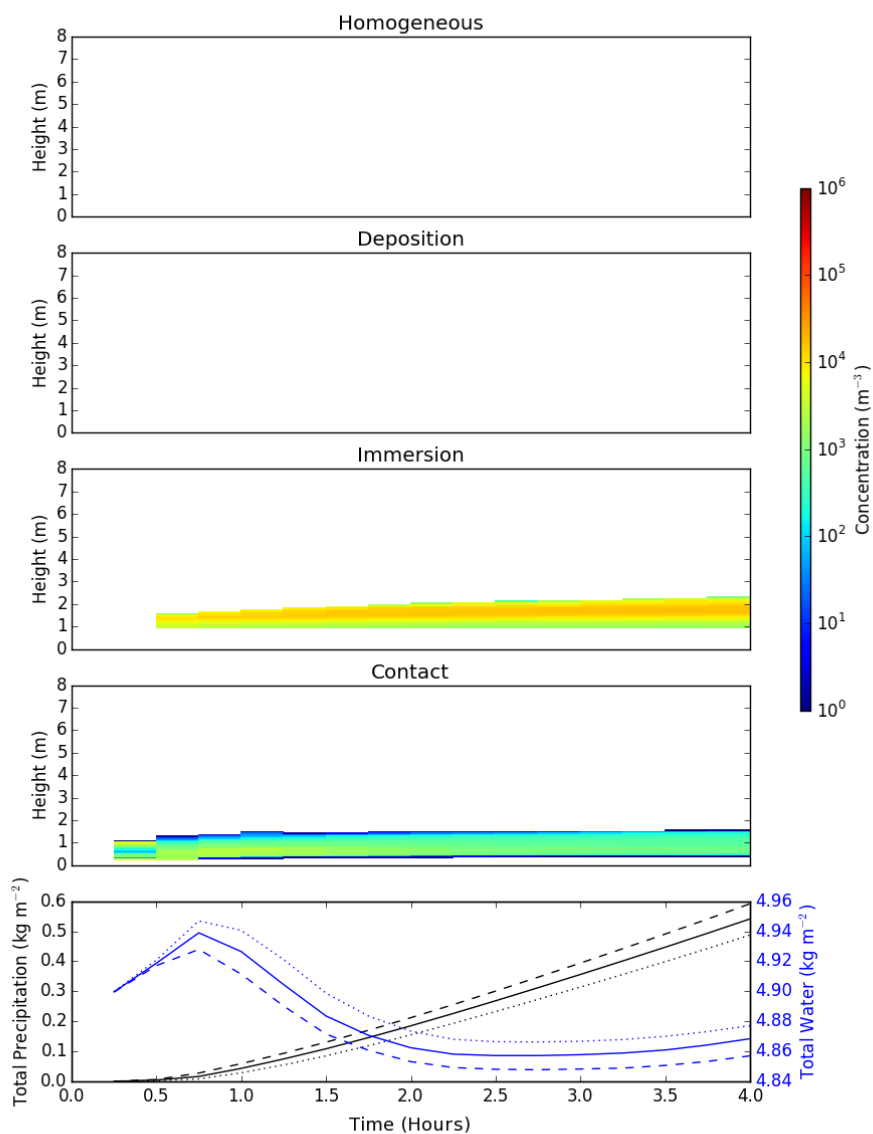


**Figure 9.** Temporal evolution of INP number concentrations in each mode for the orographic cloud. Bottom panel shows total precipitation (black) and total water (blue). Dashed (dotted) line is for the high (low) aerosol simulation.

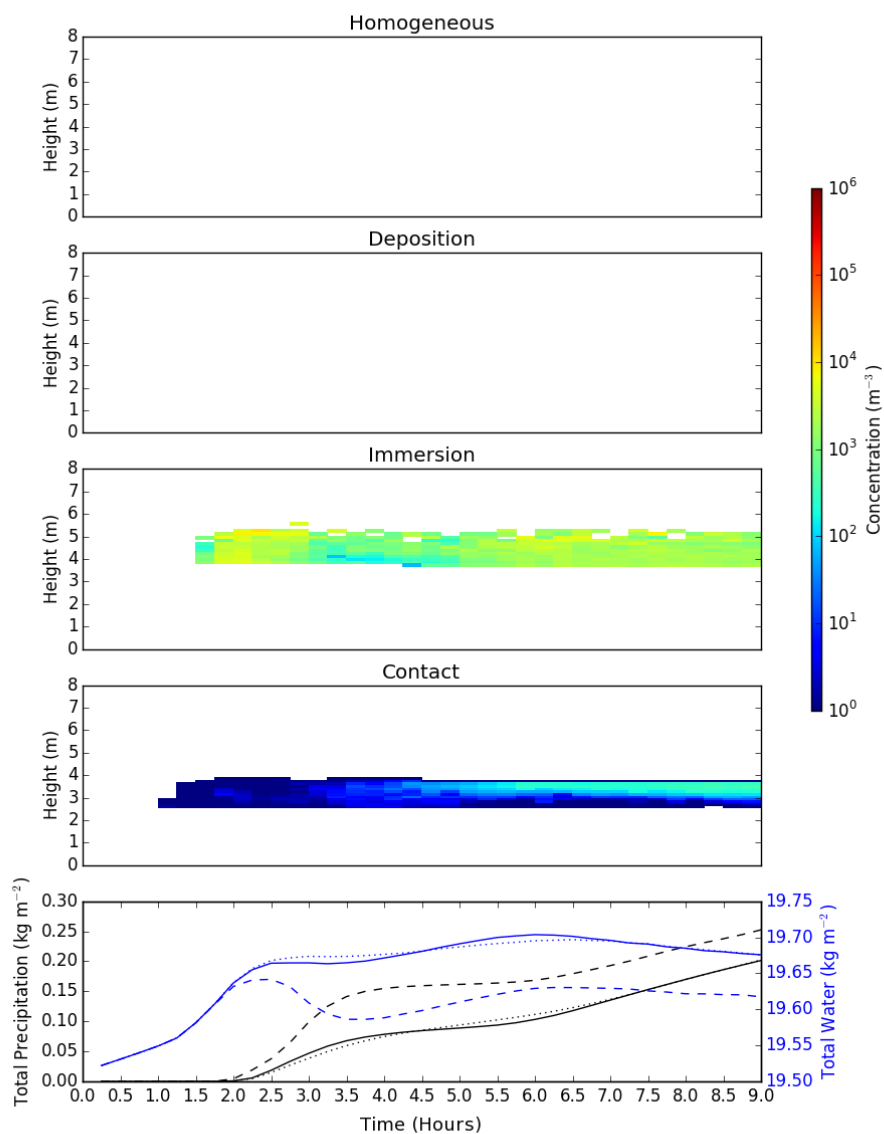


**Figure 10.** Temporal evolution of INP number concentrations in each mode for the stratiform cloud. Bottom panel shows total precipitation (black) and total water (blue). Dashed (dotted) line is for the high (low) aerosol simulation.



|                   | Hom                           | Dep                             | Imm                           | Con                             |
|-------------------|-------------------------------|---------------------------------|-------------------------------|---------------------------------|
| Heat Bubble +     | $2.94 \times 10^2$<br>(0.14)  | $2.25 \times 10^0$<br>(0.00)    | $2.02 \times 10^5$<br>(98.07) | $3.68 \times 10^3$<br>(1.79)    |
| Heat Bubble       | $2.77 \times 10^2$<br>(1.38)  | $3.11 \times 10^{-1}$<br>(0.01) | $1.76 \times 10^4$<br>(88.31) | $2.05 \times 10^3$<br>(10.30)   |
| Heat Bubble -     | $2.80 \times 10^2$<br>(8.73)  | $4.11 \times 10^{-2}$<br>(0.00) | $2.09 \times 10^3$<br>(65.07) | $8.43 \times 10^2$<br>(26.20)   |
| Deep Convective + | $3.09 \times 10^1$<br>(0.12)  | $1.47 \times 10^{-1}$<br>(0.00) | $2.37 \times 10^4$<br>(90.56) | $2.43 \times 10^3$<br>(9.32)    |
| Deep Convective   | $2.35 \times 10^2$<br>(6.56)  | $2.75 \times 10^{-1}$<br>(0.01) | $2.11 \times 10^3$<br>(58.95) | $1.24 \times 10^3$<br>(34.48)   |
| Deep Convective - | $2.51 \times 10^2$<br>(28.59) | $8.73 \times 10^{-2}$<br>(0.01) | $1.95 \times 10^2$<br>(22.18) | $4.33 \times 10^2$<br>(49.22)   |
| Orographic +      | 0<br>(0)                      | 0<br>(0)                        | $1.68 \times 10^3$<br>(85.84) | $2.76 \times 10^2$<br>(14.16)   |
| Orographic        | 0<br>(0)                      | 0<br>(0)                        | $1.21 \times 10^3$<br>(89.91) | $1.35 \times 10^2$<br>(10.09)   |
| Orographic -      | 0<br>(0)                      | 0<br>(0)                        | $7.65 \times 10^2$<br>(94.66) | $4.32 \times 10^1$<br>(5.34)    |
| Stratiform +      | 0<br>(0)                      | 0<br>(0)                        | $6.21 \times 10^2$<br>(99.97) | $1.81 \times 10^{-1}$<br>(0.03) |
| Stratiform        | 0<br>(0)                      | 0<br>(0)                        | $1.87 \times 10^2$<br>(97.54) | $4.73 \times 10^0$<br>(2.46)    |
| Stratiform -      | 0<br>(0)                      | 0<br>(0)                        | $1.85 \times 10^2$<br>(99.92) | $1.49 \times 10^{-1}$<br>(0.08) |

**Table 1.** Temporal and spatial mean INP concentrations ( $\text{m}^{-3}$ ) for each case. + (-) indicates higher (lower) dust aerosol concentrations, as shown in Figure 1. The relative contribution (%) of each mode to the total INP concentrations is shown in parenthesis.